

# A Shock-in-Jet Synchrotron Mirror Model for Blazars

*Markus Böttcher*  
*North-West University*  
*Potchefstroom, South Africa*

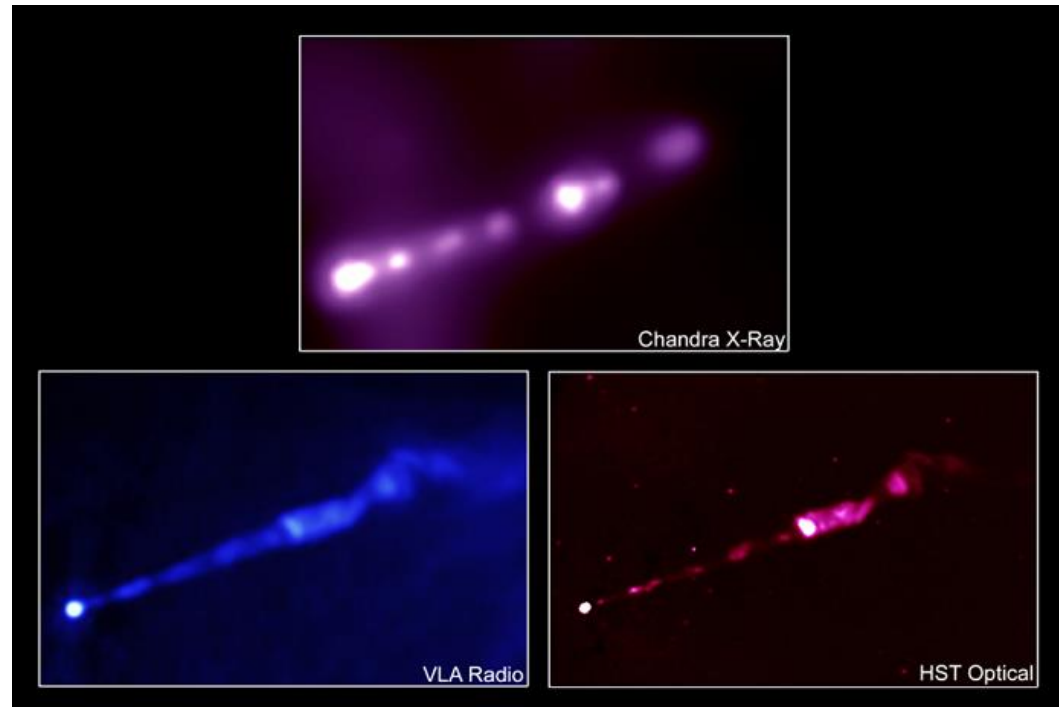


Supported by the South African Research Chairs Initiative (SARChI) of the Department of Science and Technology and the National Research Foundation of South Africa.

# Relativistic Shocks in Jets

- Internal Shocks: likely sites of relativistic particle acceleration.
- Most likely mildly relativistic,  $\beta\gamma \sim 1$
- Efficient Diffusive Shock Acceleration at mildly relativistic, oblique shocks produces relativistic, non-thermal electron distributions which can be as hard as  $n_e(\gamma) \sim \gamma^{-1}$ , depending on obliquity and efficiency of pitch-angle scattering.

Jet of M87 at different wavelengths



# Time-Dependent Electron Evolution with Radiative Energy Losses

Acceleration time scale:

$$t_{acc} = \eta t_{gyr} = \eta \frac{2\pi \gamma m_e c}{eB} \ll t_{cool}, t_{dyn}$$

For almost all electrons

⇒ Use shock-accelerated electron spectrum (MC simulations of DSA by Summerlin & Baring 2012) as instantaneous injection  $Q_e(\gamma)$ ;

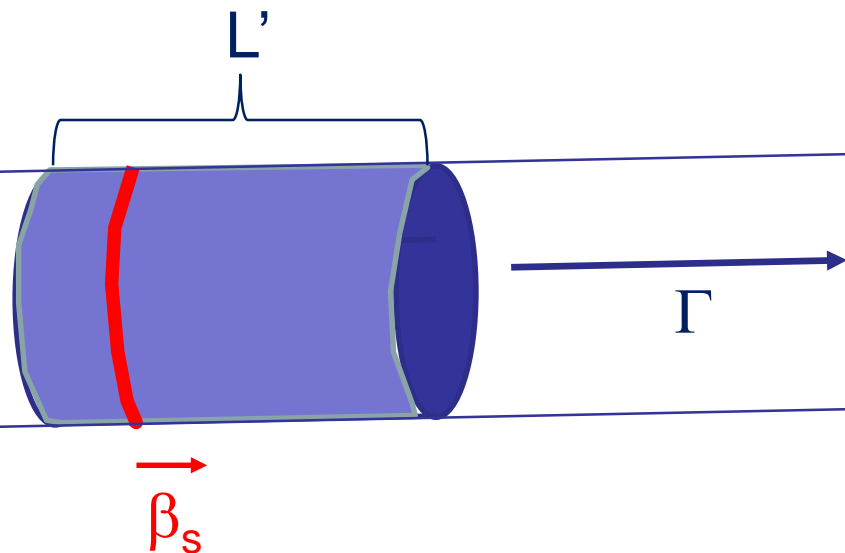
⇒ Solve Fokker-Planck Equation for electrons:

$$\frac{\partial n_e(\gamma, t)}{\partial t} = - \frac{\partial}{\partial \gamma} (\dot{\gamma} n_e) + Q_e(\gamma, t) - \frac{n_e(\gamma, t)}{t_{esc, e}}$$

# Numerical Scheme

- Injection spectra from turbulence characteristics + MC simulations of DSA
- Injection from small acceleration zone (shock) into larger radiation zone
- Time-dependent leptonic code based on Böttcher & Chiang (2002)
- Radiative processes:
  - Synchrotron
  - Synchrotron self-Compton (SSC)
  - External Compton (EC: dust torus + BLR + direct accretion disk)

Shock injection “on” for  
 $0 < \Delta t' < L'/v'_s$



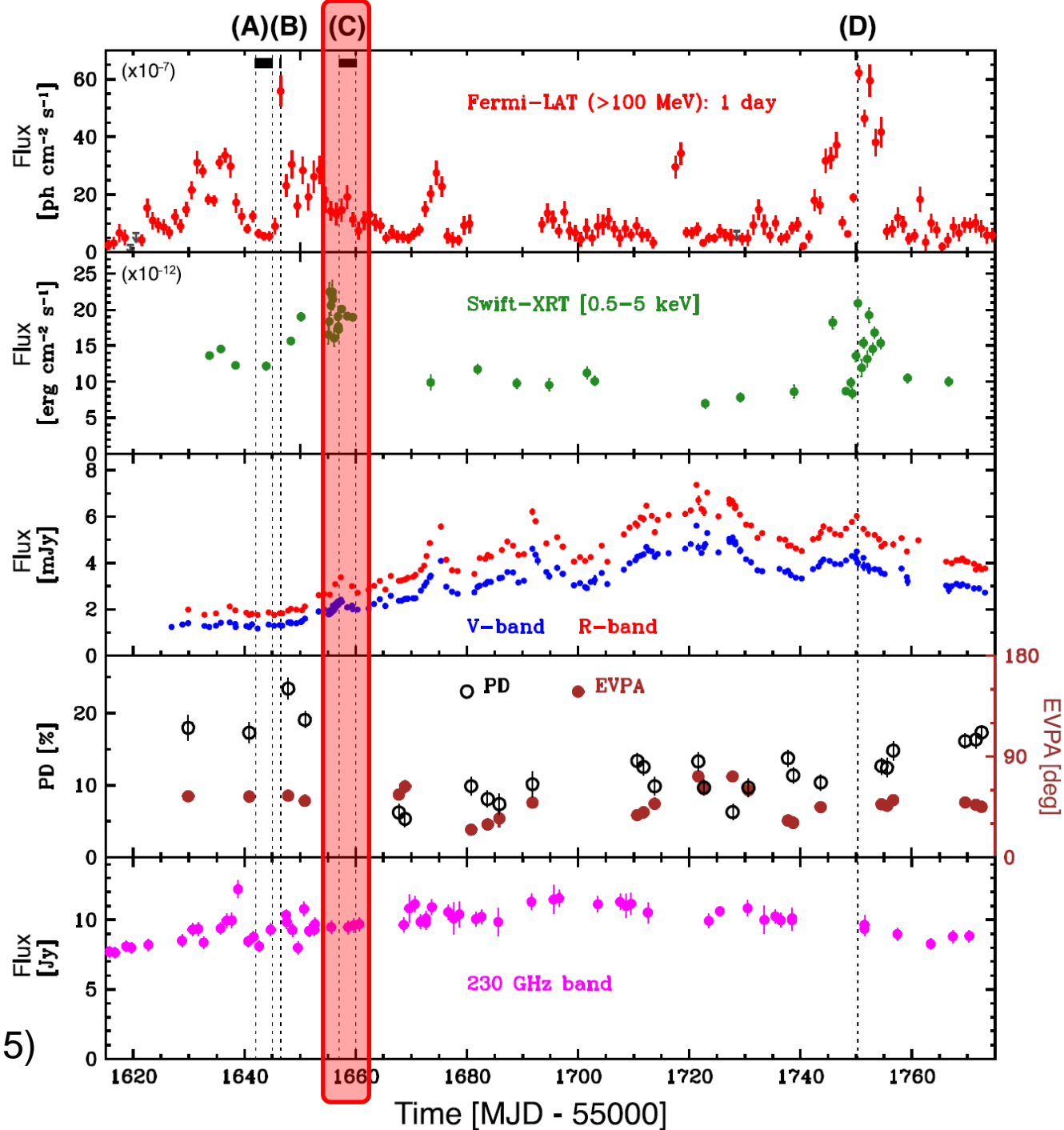
$$Q_{e,s}(\gamma, t') = Q_{e,s}(\gamma) H(t'; 0, \Delta t')$$

# Example: FSRQ 3C279

Extended  
flaring period  
2013 – 2014

Variability  
time scale  
~ 1 day

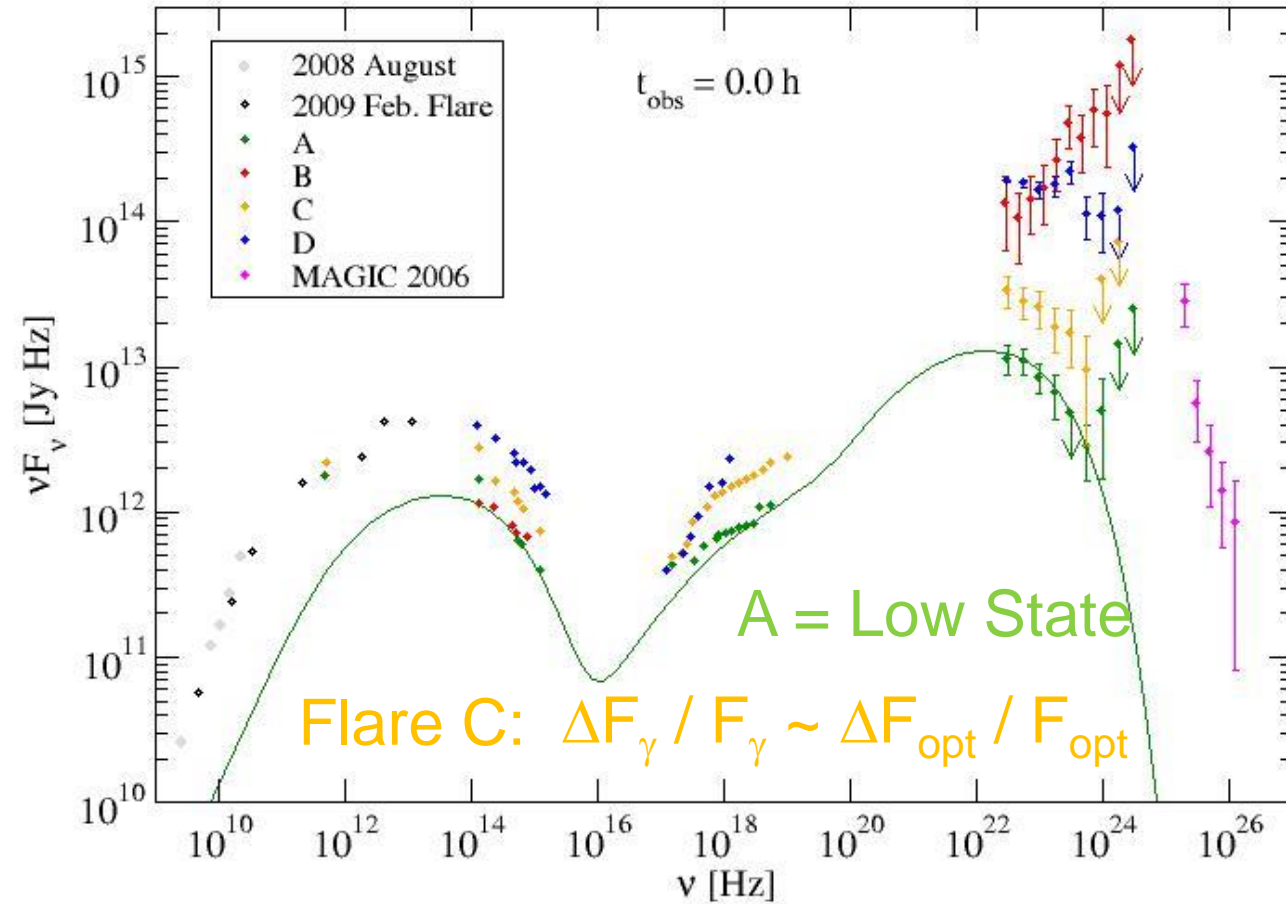
(Hayashida et al. 2015)



# Example: FSRQ 3C279 (2013 – 2014)

$$\lambda_{\text{pas}} = 300 r_g \gamma^2$$

3C279  
(Hayashida et al. 2015)



$$\eta_1 = 300$$

$$\alpha = 3$$

$$B = 0.65 \text{ G}$$

$$\delta = 15$$

$$R = 1.8 \cdot 10^{16} \text{ cm}$$

$$\rightarrow \Delta t' \sim \text{few} \cdot 10^5 \text{ s}$$

$$\rightarrow \Delta t_{\text{obs}} \sim \text{few hr}$$

$\gamma$ -rays EC (Dust Torus) dominated:

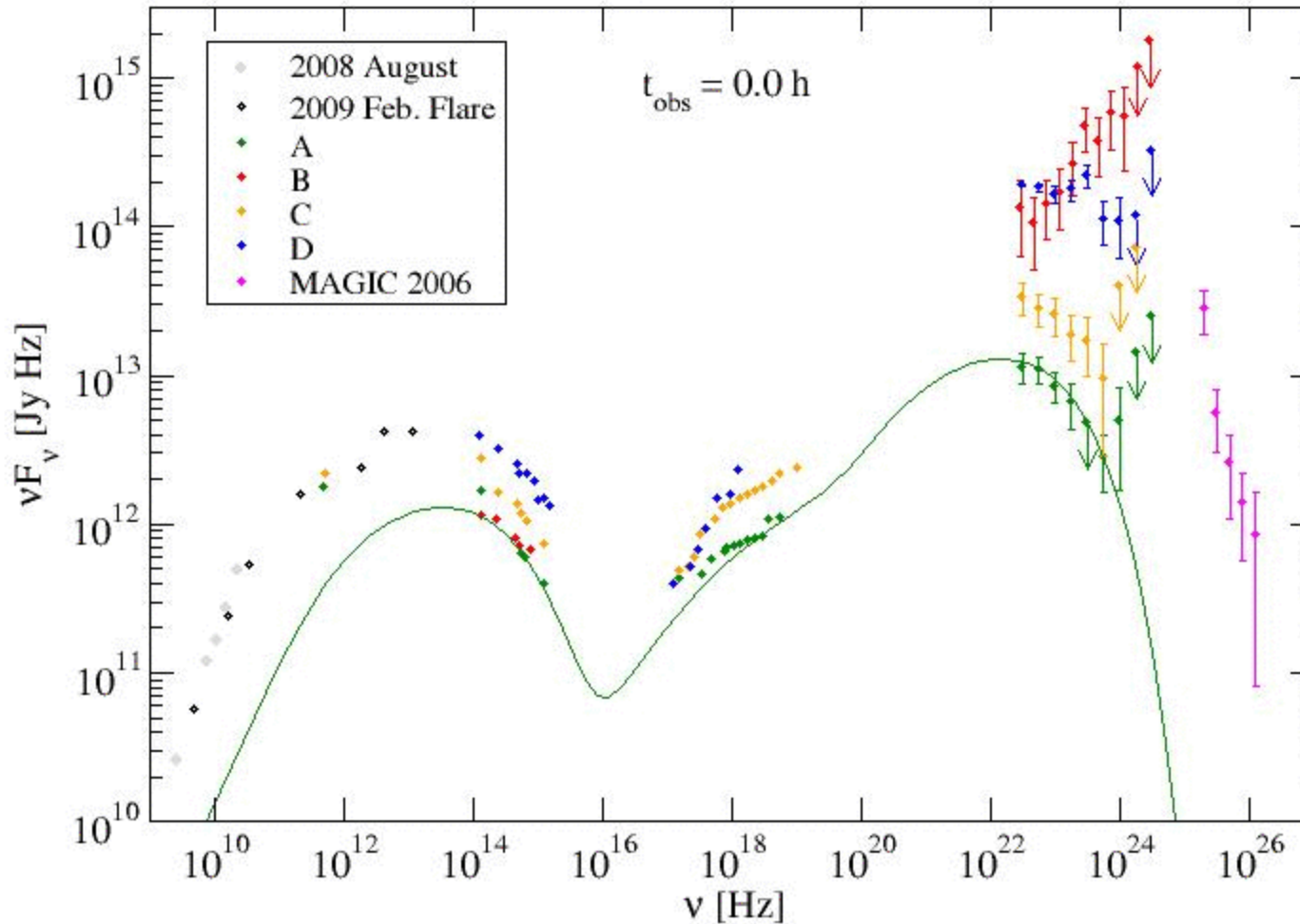
$$u = 4 \cdot 10^{-4} \text{ erg/cm}^3$$

$$T_{\text{BB}} = 300 \text{ K}$$

(Böttcher & Baring 2019)

# 3C279 – Flare C

3C279  
(Hayashida et al. 2015)



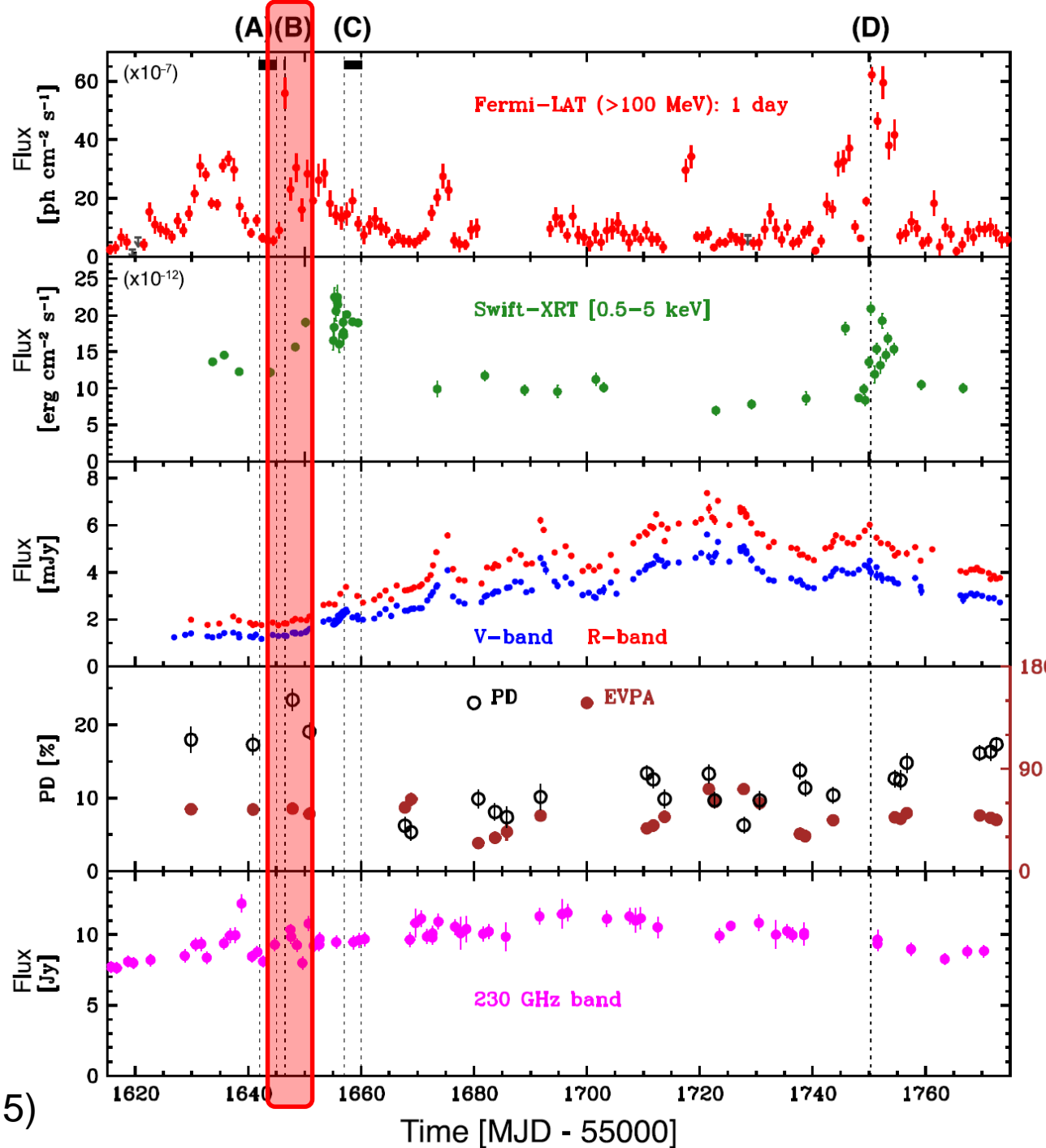
Flare modeled with

$$L_{\text{inj}} = 1.1 \times 10^{43} \\ \rightarrow 5.0 \times 10^{43} \text{ erg/s}$$

(Böttcher & Baring 2019)

# Example: FSRQ 3C279

Flare B  
(December 2013):  
Orphan  $\gamma$ -ray flare



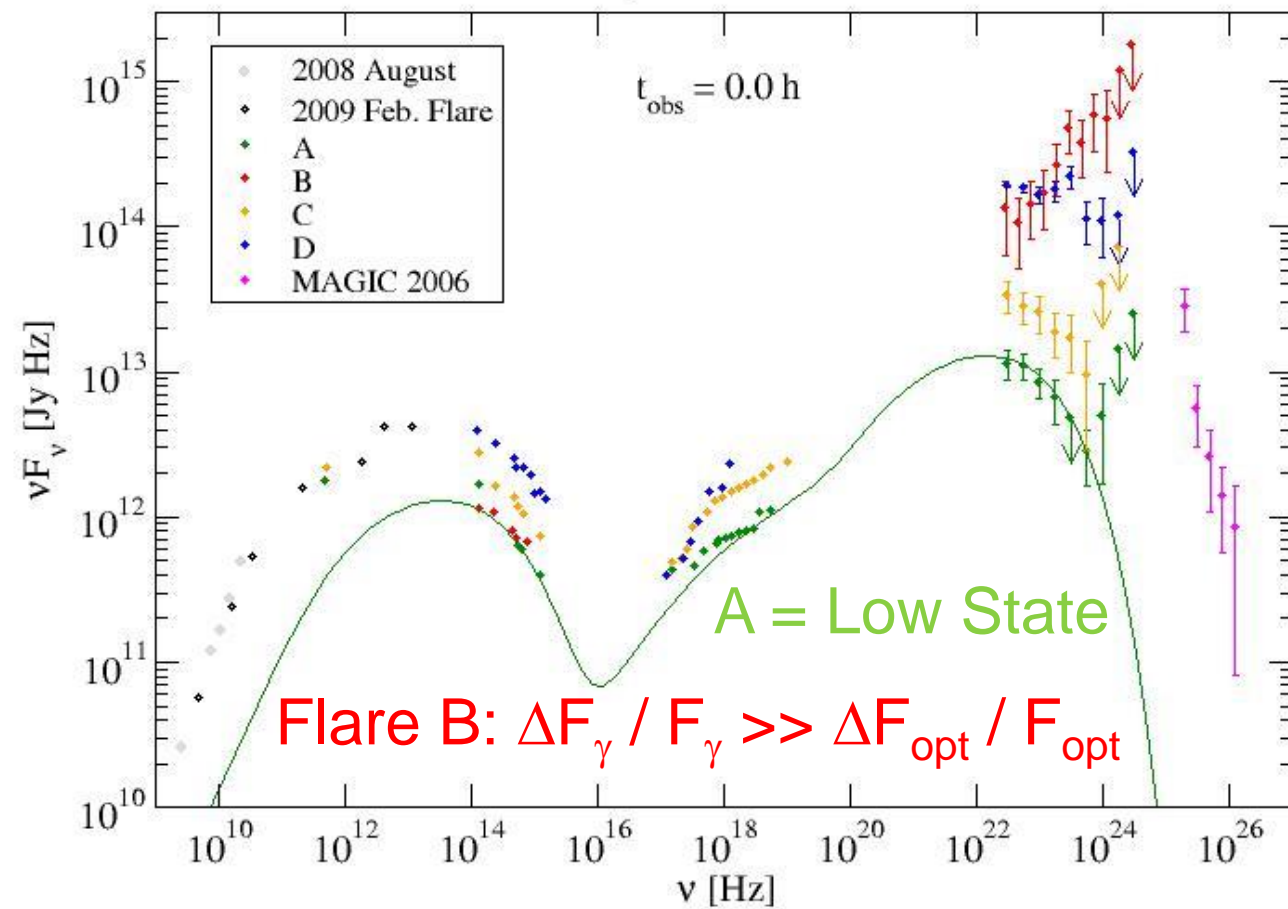
(Hayashida et al. 2015)



# Example: FSRQ 3C279 (2013 – 2014)

$$\lambda_{\text{pas}} = 300 r_g \gamma^2$$

3C279  
(Hayashida et al. 2015)



(Böttcher & Baring 2019)

$$\eta_1 = 300$$

$$\alpha = 3$$

$$B = 0.65 \text{ G}$$

$$\delta = 15$$

$$R = 1.8 \cdot 10^{16} \text{ cm}$$

$$\rightarrow \Delta t' \sim \text{few} \cdot 10^5 \text{ s}$$

$$\rightarrow \Delta t_{\text{obs}} \sim \text{few hr}$$

$\gamma$ -rays EC (Dust  
Torus) dominated:

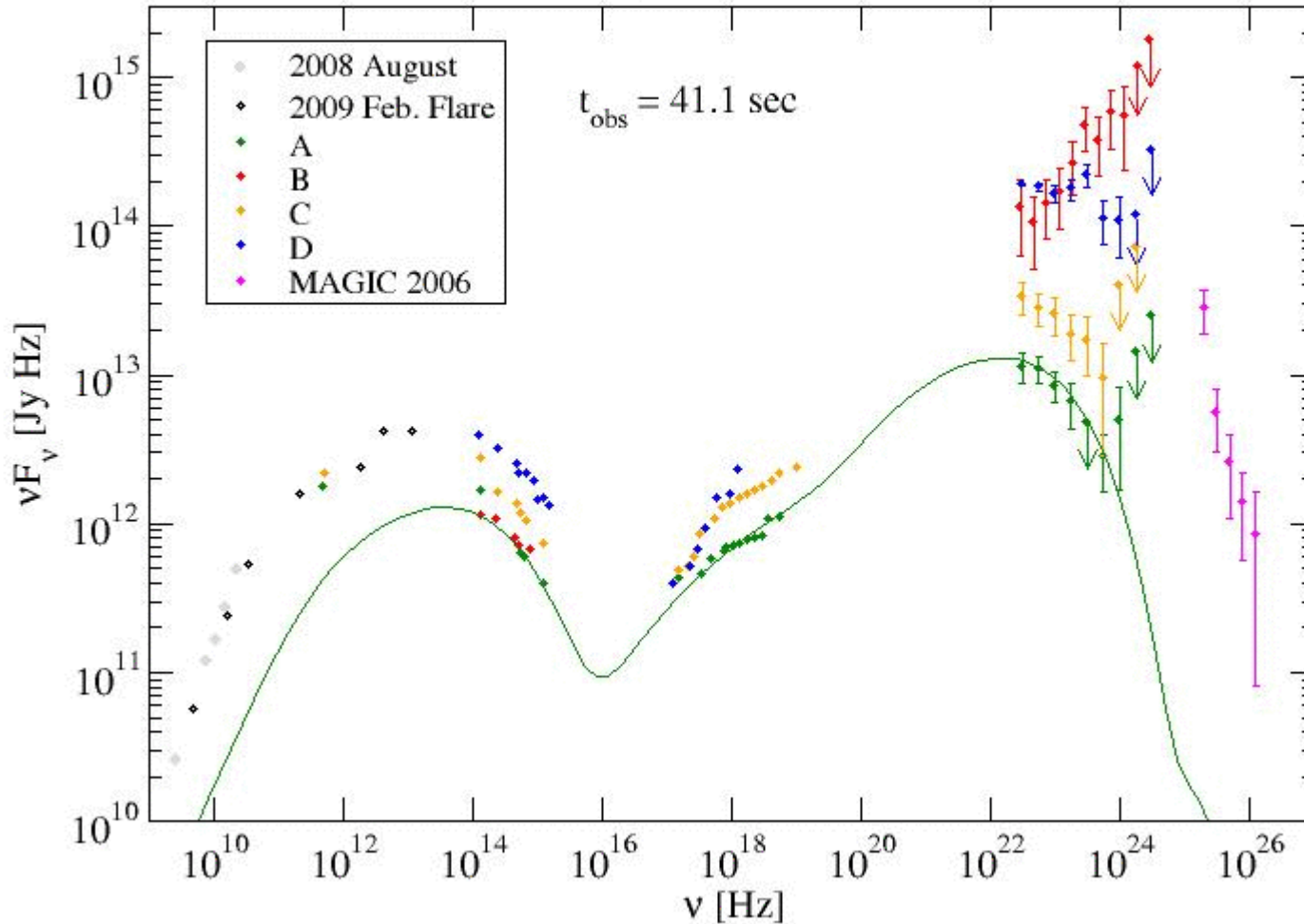
$$u = 4 \cdot 10^{-4} \text{ erg/cm}^3$$

$$T_{\text{BB}} = 300 \text{ K}$$

# 3C279 – Flare B

3C279

(Hayashida et al. 2015)



Flare modeled with

$$L_{\text{inj}} = 1.1 \times 10^{43} \rightarrow 4.0 \times 10^{44} \text{ erg/s}$$

$$\eta_1 = 100 \rightarrow 10$$

$$\alpha = 3.0 \rightarrow 2.3$$

$\Rightarrow$  Harder electron spectrum

$$B = 0.65 \rightarrow 0.075$$

with gradual recovery after shock passage:

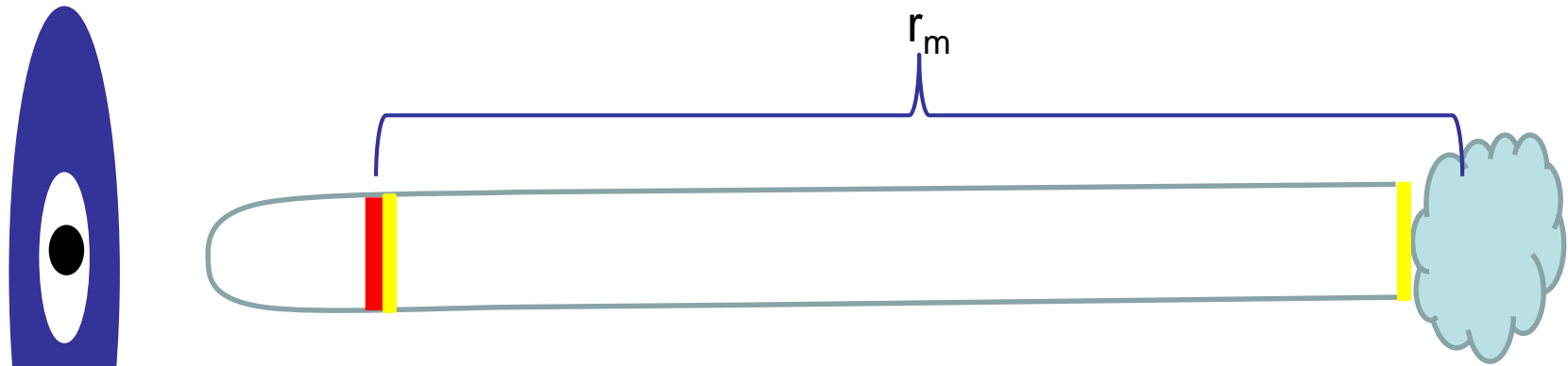
(Böttcher & Baring 2019)

$$B(t) = B_q + (B_f - B_q) e^{-(t' - t'_{\text{end}})/t'_{\text{rec}}}, \quad t' > t'_{\text{end}}$$

# Alternative Idea: Synchrotron Mirror

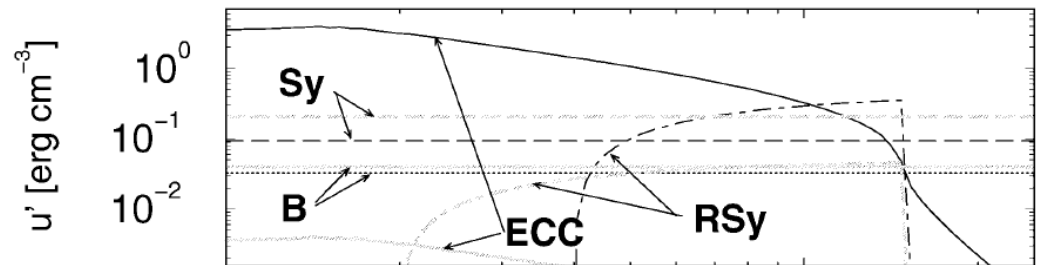
Originally proposed by Ghisellini & Madau (1996); Böttcher & Dermer (1998);  
Bednarek (1998);

further developed by Vittorini et al. 2014; Tavani et al. 2015)



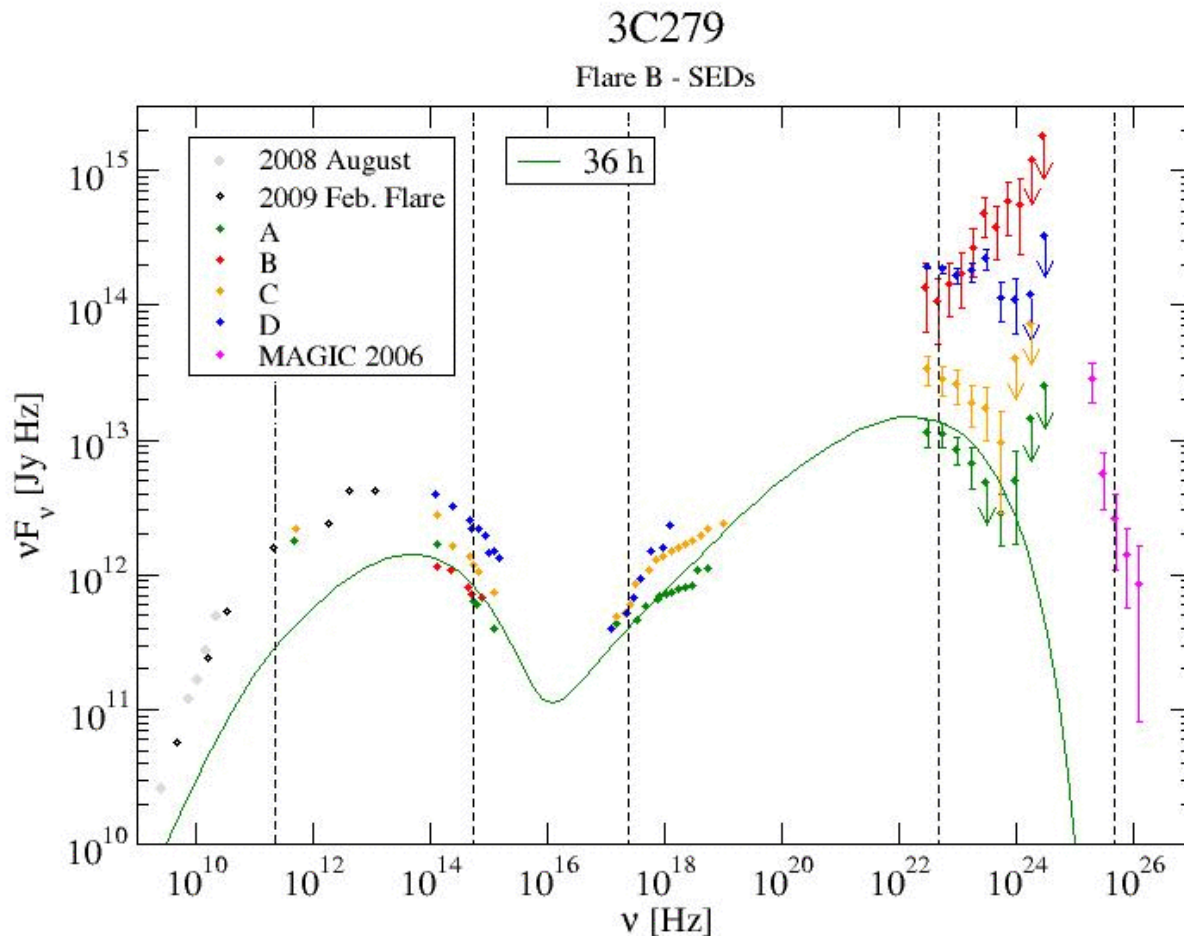
Short enhancement  
of external radiation  
field on observed  
time scale

$$\Delta t_{obs} \sim \frac{r_m}{8 \Gamma^4 c}$$



(Böttcher & Dermer 1998)

# 3C279 Flare B with the Synchrotron Mirror Model?



Keeping all shock parameters constant:

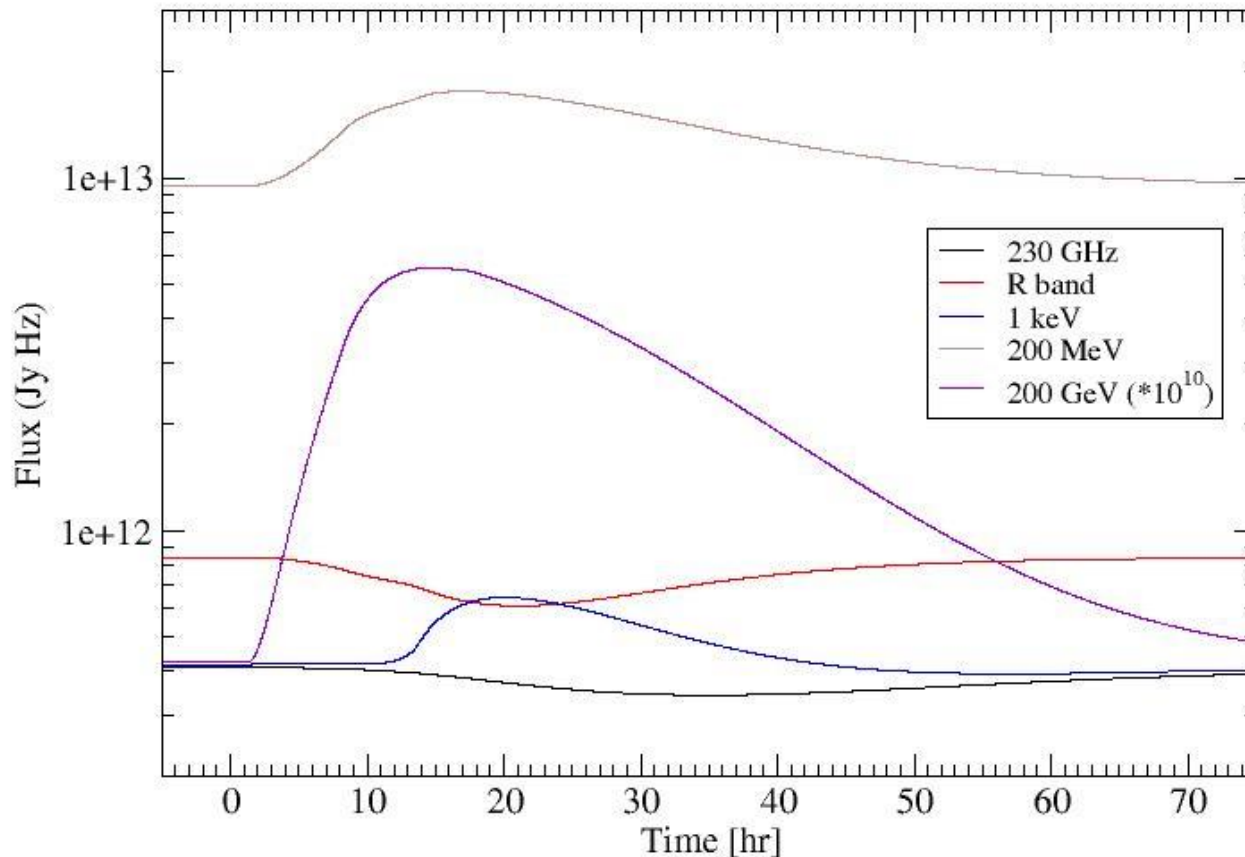
Only moderate orphan flare, irrespective of mirror parameters, due to limited energy budget.

Impossible to reproduce large orphan flare (Flare B)

Suppression of synchrotron emission due to increased radiative cooling.

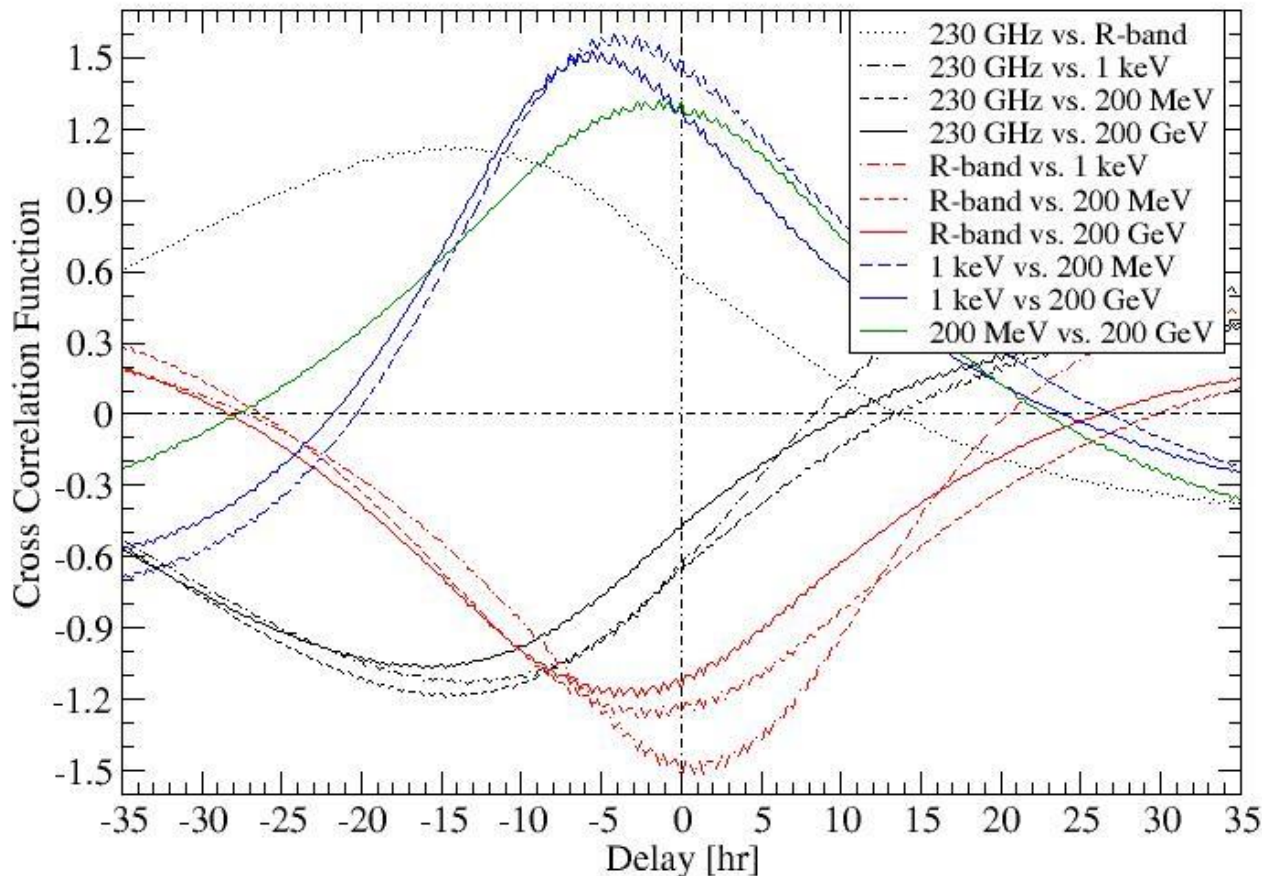
# Spectral Variability Features of the Shock-in-Jet Synchrotron Mirror Model

## Multi-wavelength lightcurves



# Spectral Variability Features of the Shock-in-Jet Synchrotron Mirror Model

## Cross-Correlations

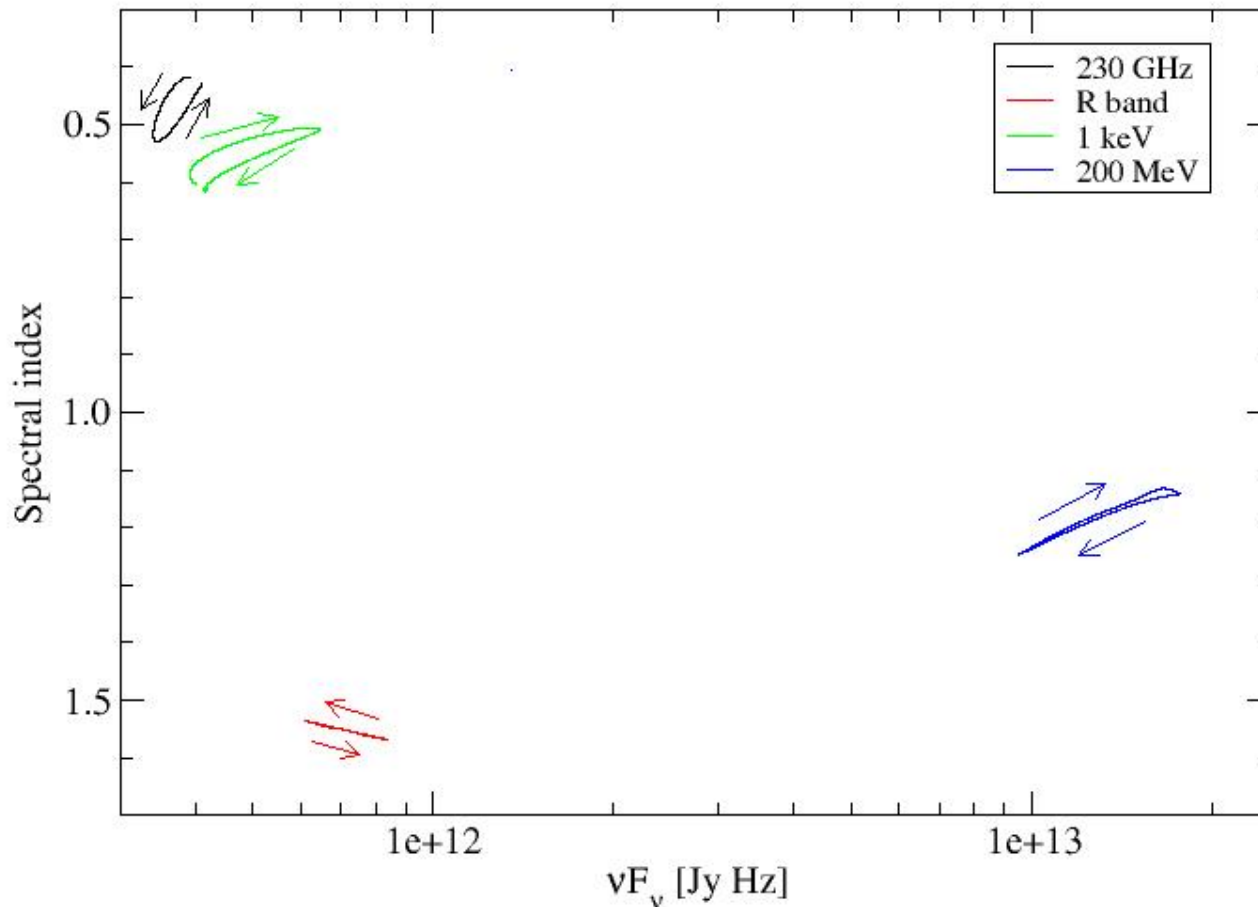


Radio and optical  
anti-correlated with  
X-ray and  $\gamma$ -ray  
emission.

Radio dip delayed  
by  $\sim 10 - 20$  hr  
behind flares / dips  
in other wavebands.

# Spectral Variability Features of the Shock-in-Jet Synchrotron Mirror Model

## Hardness-Intensity Diagrams



No significant spectral hysteresis in any waveband.

Harder-when-brighter trend in all wavebands, except optical (synchrotron).



# Summary

1. Time-dependent, coupled MC Simulations of Diffusive Shock Acceleration and radiation transport: Naturally capable of reproducing MWL flares with roughly equal flare amplitude in synchrotron and Compton SED components (e.g., flare C of 3C279 in 2013).
2. Flares with strongly increased Compton dominance (incl. orphan  $\gamma$ -ray flares, e.g. flare B of 3C279 in 2013) require fine-tuned B-field evolution to avoid simultaneous synchrotron flares.
3. Alternative interpretation through synchrotron mirror scenario plausible, but without increased energy input into electrons, only moderate orphan flares can be produced.
4. Significant anti-correlations between synchrotron (radio – optical) and Compton (X-rays –  $\gamma$ -rays) with radio time lags of  $\sim 10 - 20$  hours.
5. No significant spectral hysteresis, with harder-when brighter trend in most wavebands, except optical.





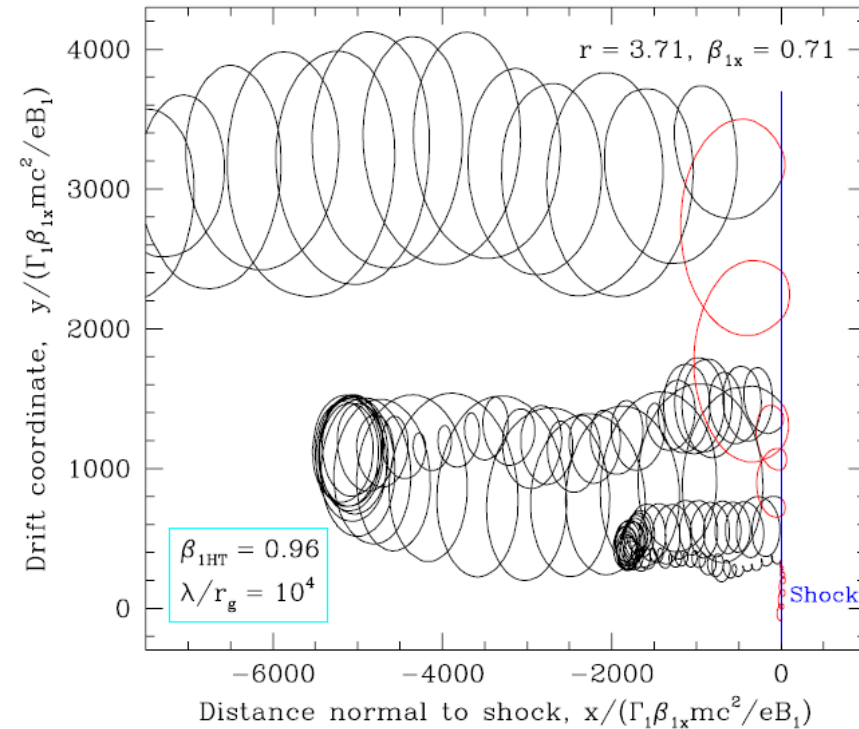
# Thank you!

Any opinion, finding and conclusion or recommendation expressed in this material is that of the authors and the NRF does not accept any liability in this regard.

# Backup Slides

# Monte-Carlo Simulations of Diffusive Shock Acceleration (DSA)

- Gyration in B-fields and diffusive transport (pitch-angle diffusion) modeled by a Monte Carlo technique.
- Shock crossings produce net energy gains → first-order Fermi.

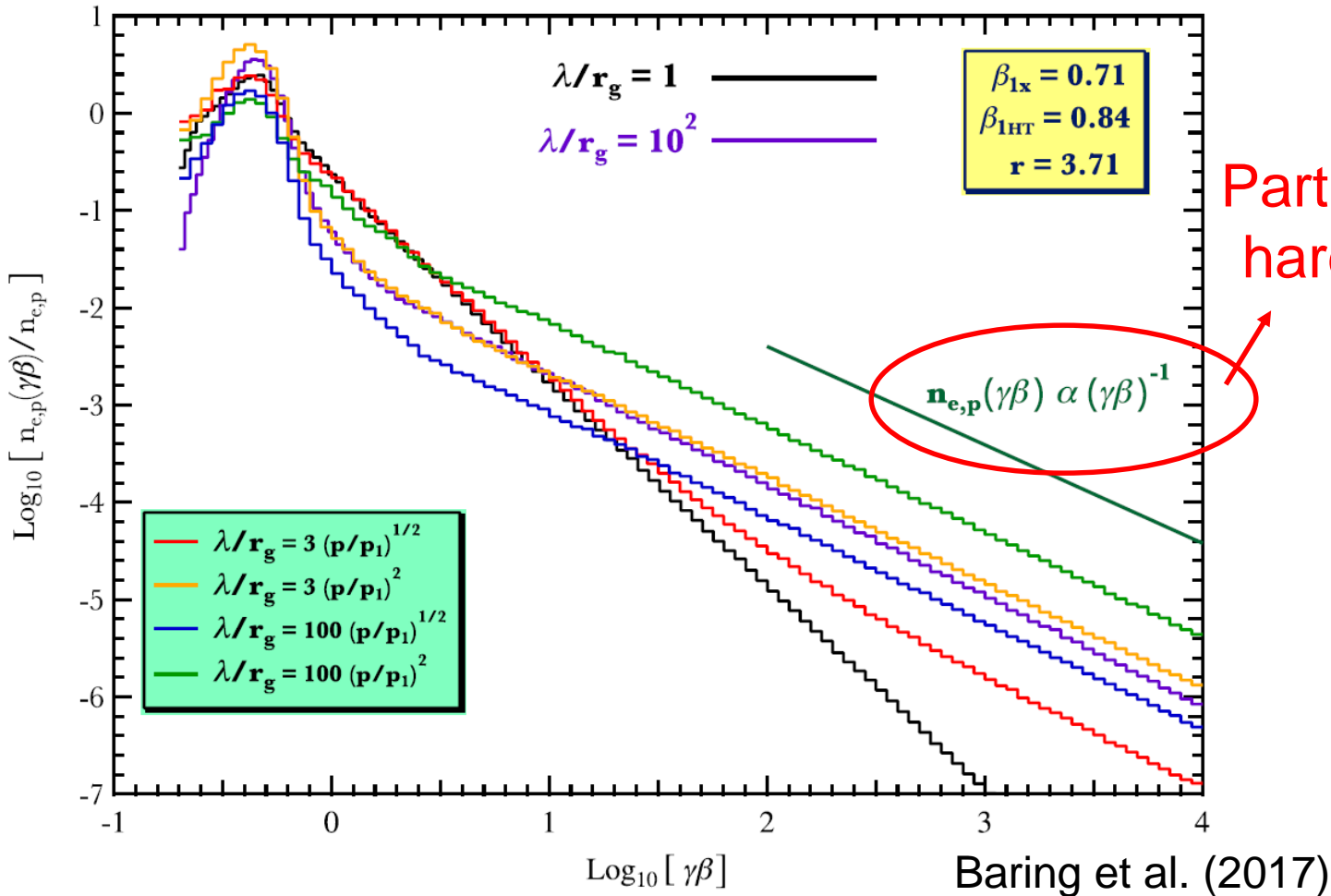


(Summerlin & Baring 2012)

- Pitch-angle diffusion parameterized through a mean-free-path ( $\lambda_{pas}$ ) parameter  $\eta$  ( $p$ ):

$$\lambda_{pas} = \eta(p) * r_g \sim p^\alpha \quad (\alpha \geq 1)$$

# Shock Acceleration Spectra

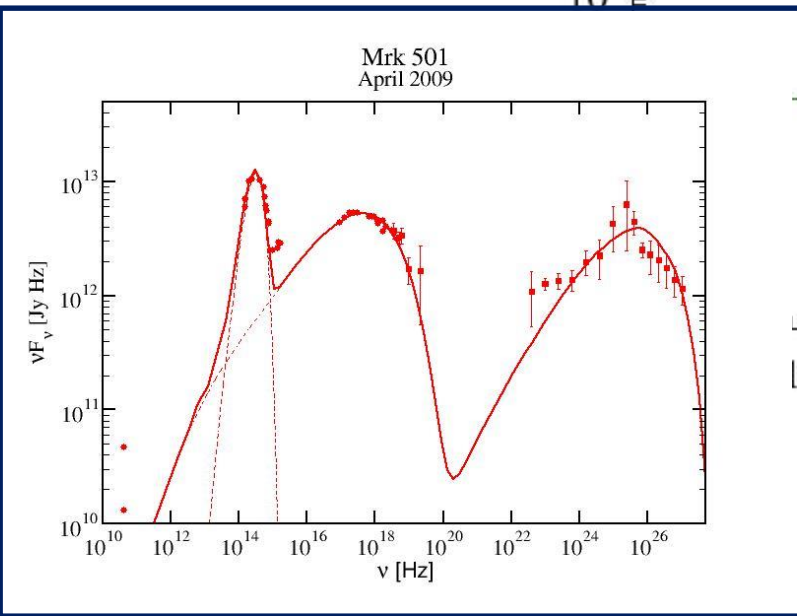
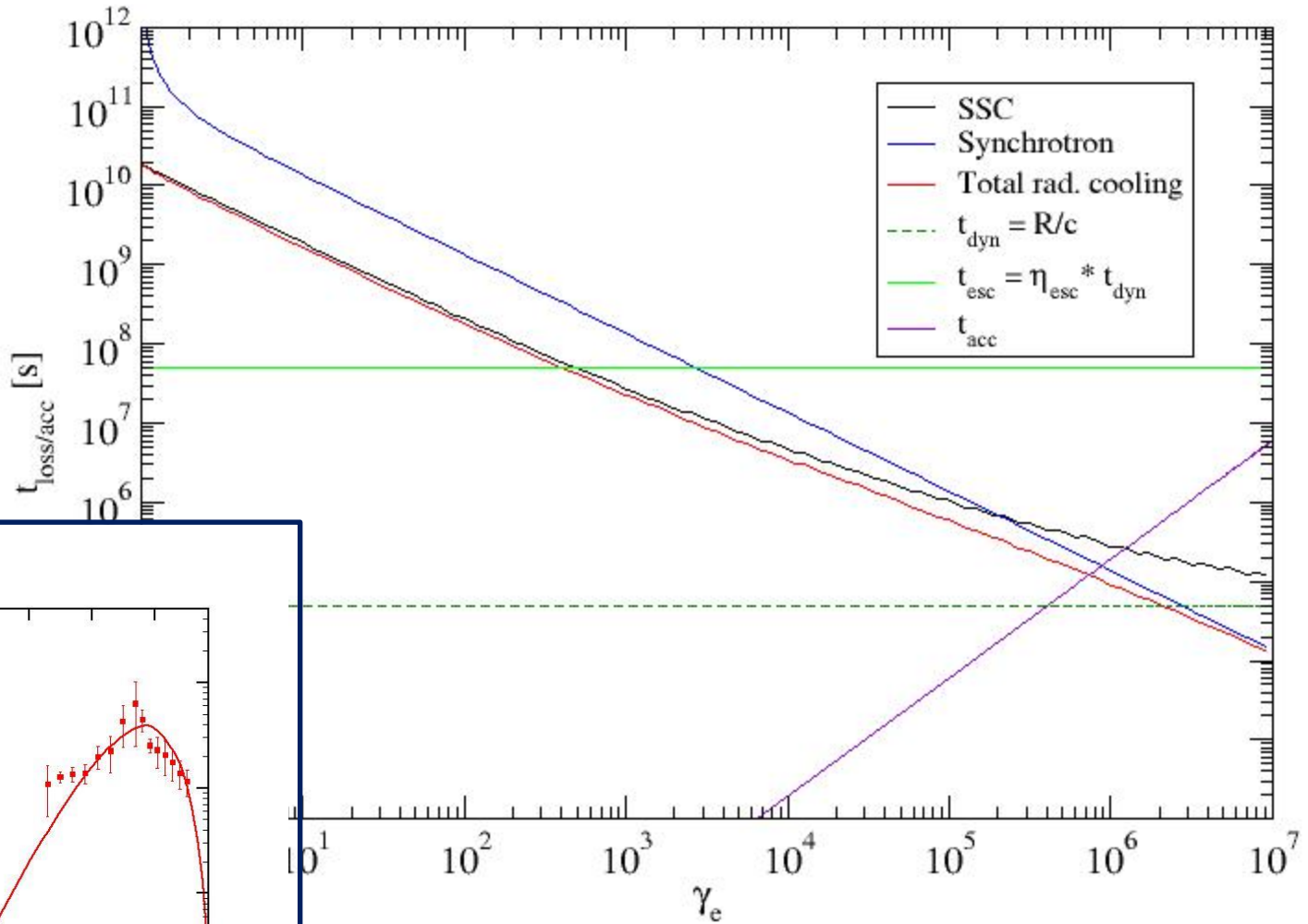


Particle spectra as hard as  $n(\gamma) \sim \gamma^{-1}$  possible!

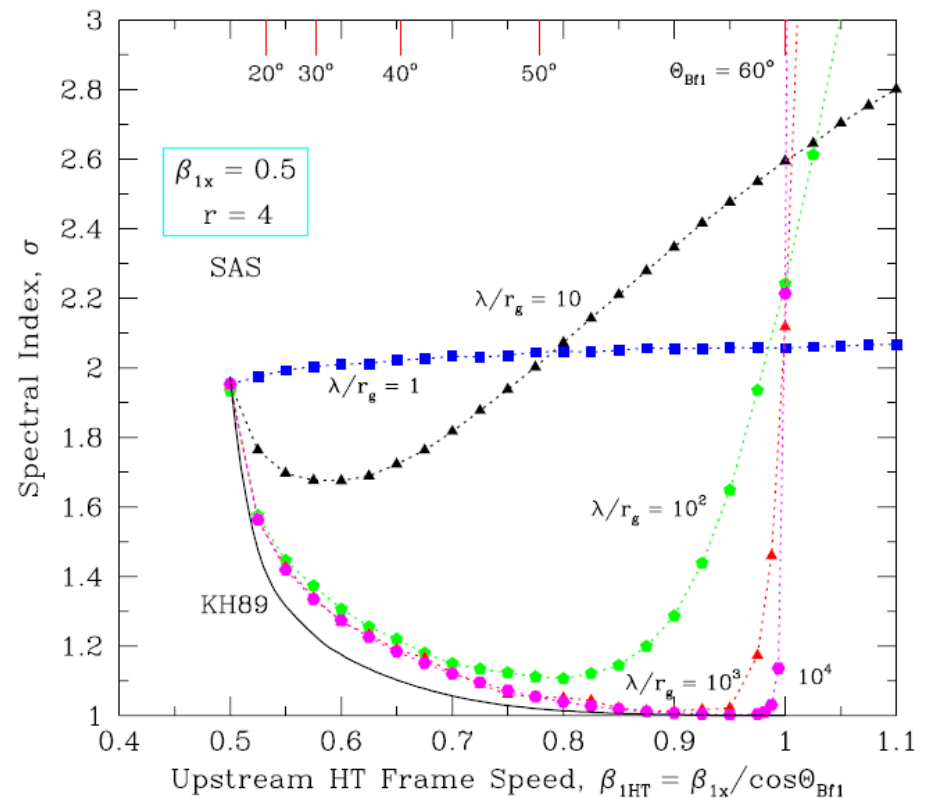
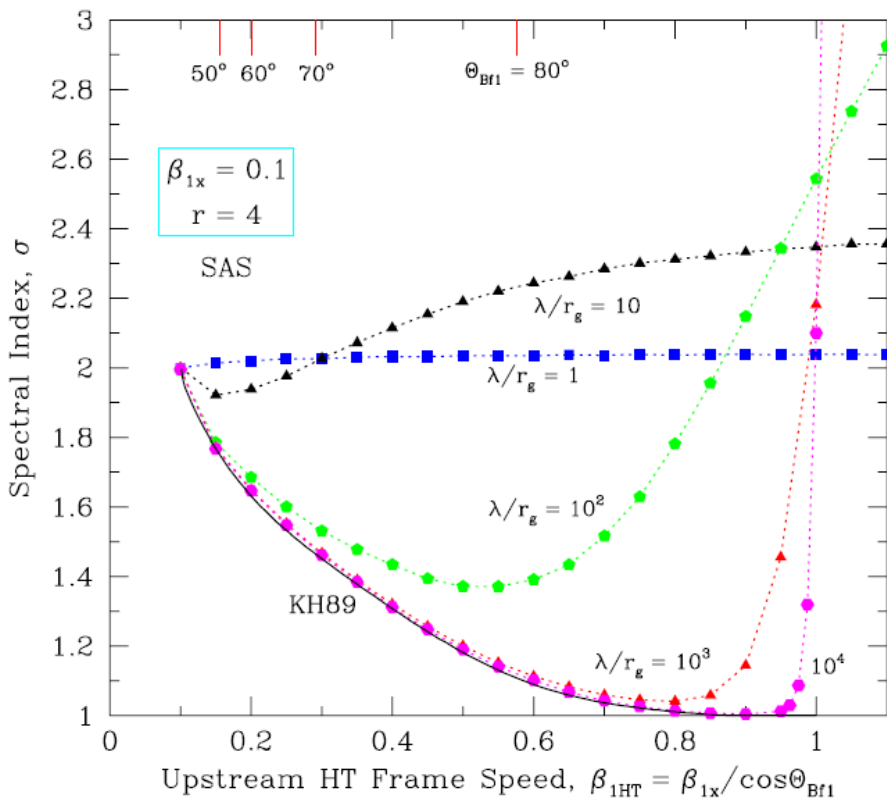
Non-thermal particle spectral index and thermal-to-non-thermal normalization are strongly dependent on  $\eta_0$ ,  $\alpha$ , and B-field obliquity!

# Electron Evolution Time Scales

Mrk 501



# Acceleration Indices for Oblique Shocks



(Summerlin & Baring 2012)

- Non-thermal spectra as hard as  $n(p) \sim p^{-1}$  achievable for moderately sub-luminal shocks.

# Constraints from Blazar SEDs

Synchrotron peak  $\leftrightarrow \gamma_{\max}$

Balance  $t_{\text{acc}} \sim \eta(\gamma) \omega_{\text{gyr}}(\gamma)^{-1}$   
with radiative cooling time scale

If synchrotron cooling dominates:

$$\gamma_{\max} \sim B^{-1/2} [\eta(\gamma_{\max})]^{-1/2}$$

$$\Rightarrow h\nu_{\text{sy}} \sim 100 \delta [\eta(\gamma_{\max})]^{-1} \text{ MeV} \quad (\text{independent of B-field!})$$

# Constraints from Blazar SEDs

$$h\nu_{\text{sy}} \sim 100 \delta [\eta(\gamma_{\text{max}})]^{-1} \text{ MeV} \quad (\text{independent of B-field!})$$

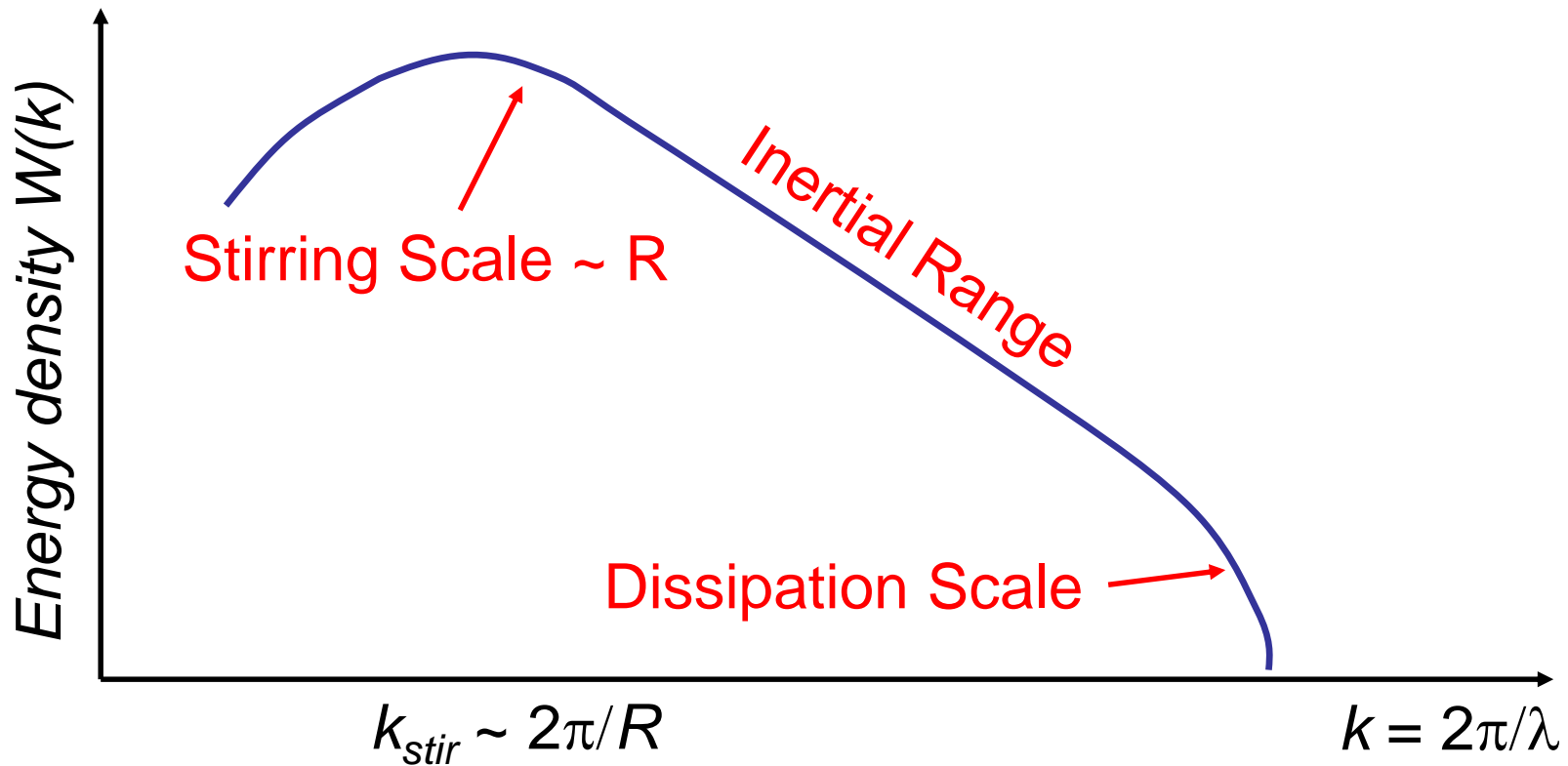
- ⇒ Need large  $\eta(\gamma_{\text{max}})$  to obtain synchrotron peak in optical/UV/X-rays
- ⇒ But: Need moderate  $\eta(\gamma \sim 1)$  for efficient injection of particles into the non-thermal accelerations scheme
- ⇒ Need strongly energy dependent pitch-angle scattering m.f.p., with  $\alpha > 1$  (Baring et al. 2017)



# Implications for Shock-Induced Turbulence

Gyro-resonance condition:  $\lambda_{res} \propto \rho$

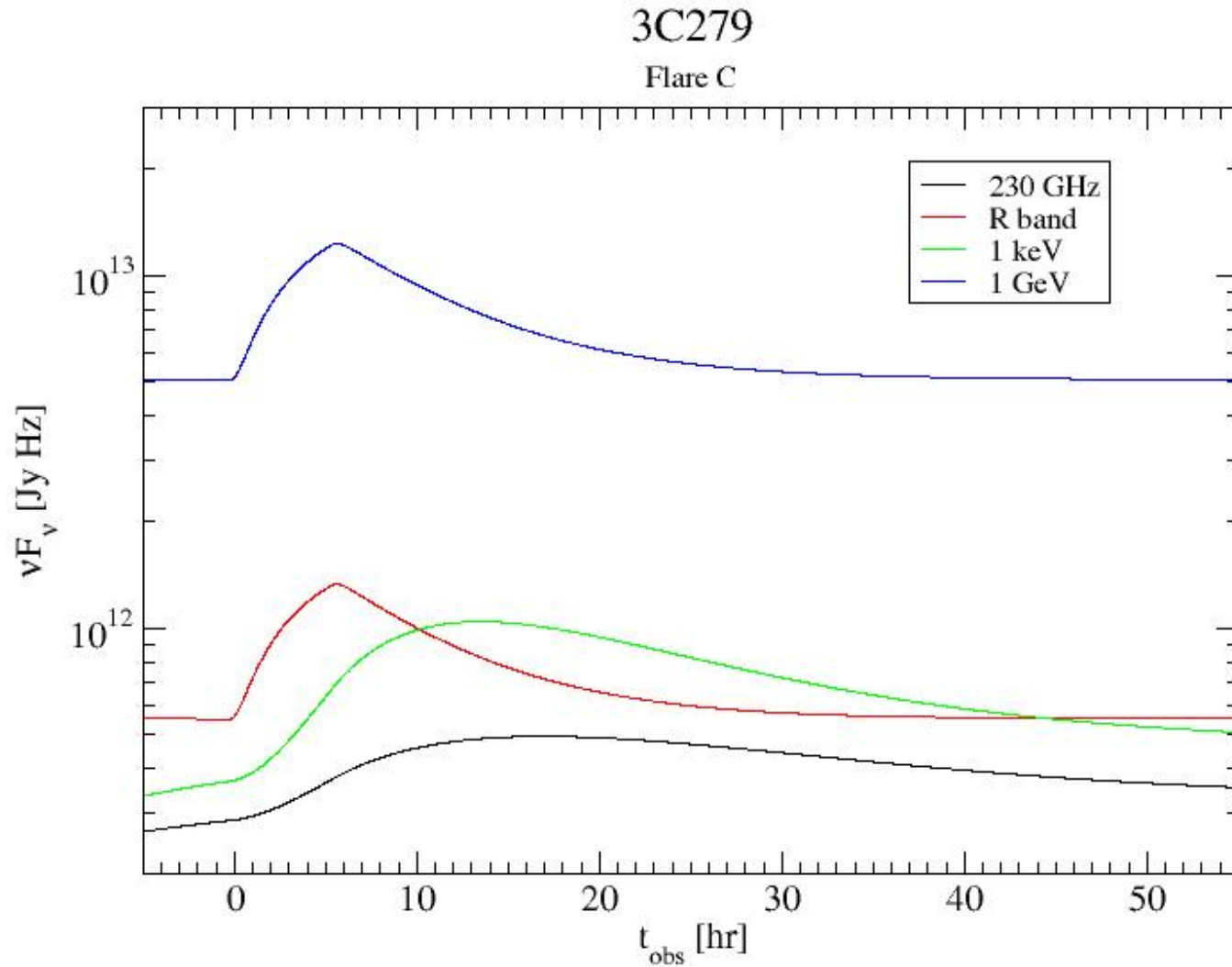
=> Higher-energy particles interact with longer-wavelength turbulence



Turbulence level decreasing with increasing distance from the shock  
=> High-energy (large  $r_g$ ) particles "see" reduced turbulence  
=> Large  $\lambda_{pas}$

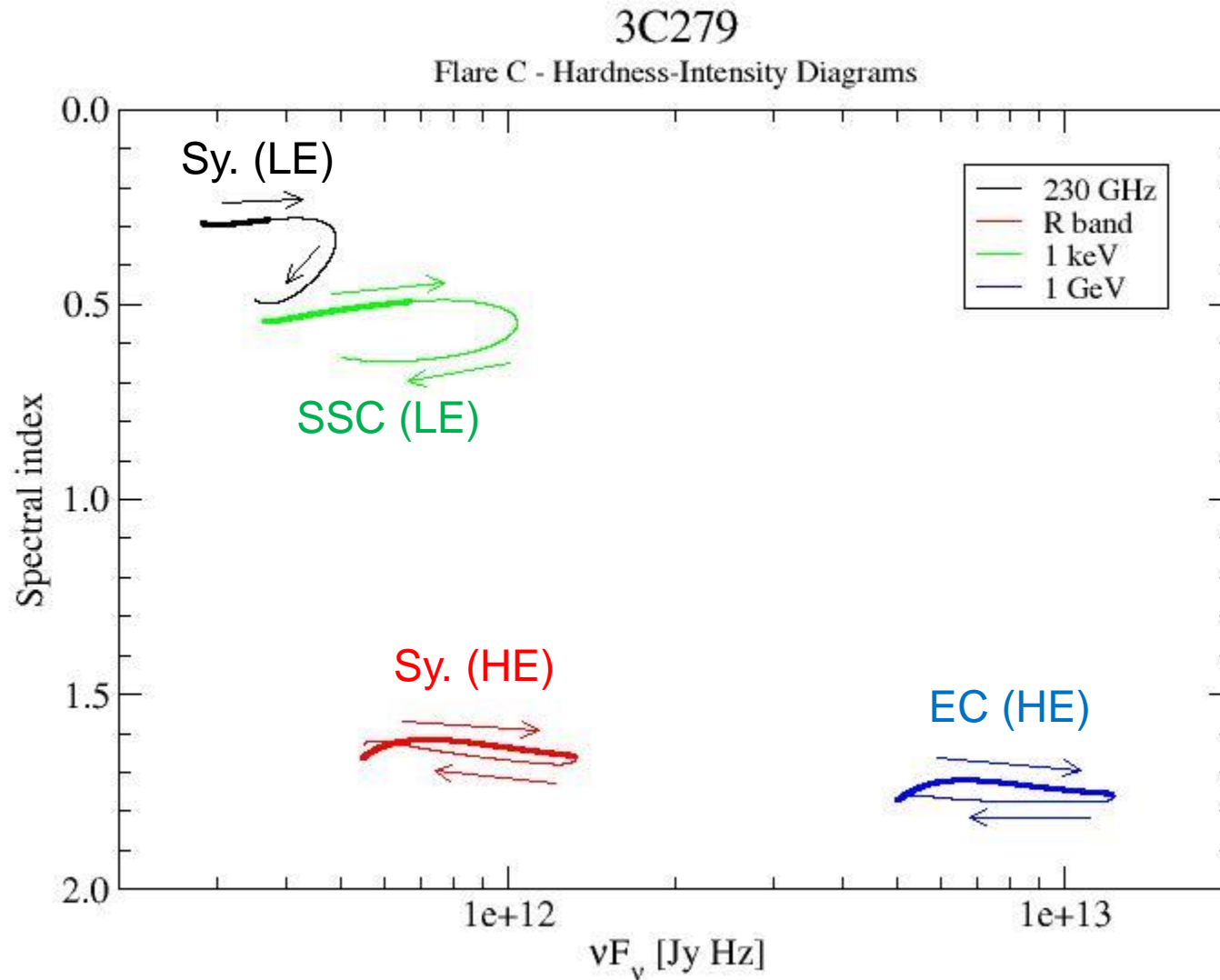
# 3C279 – Flare C

## Model Light Curves



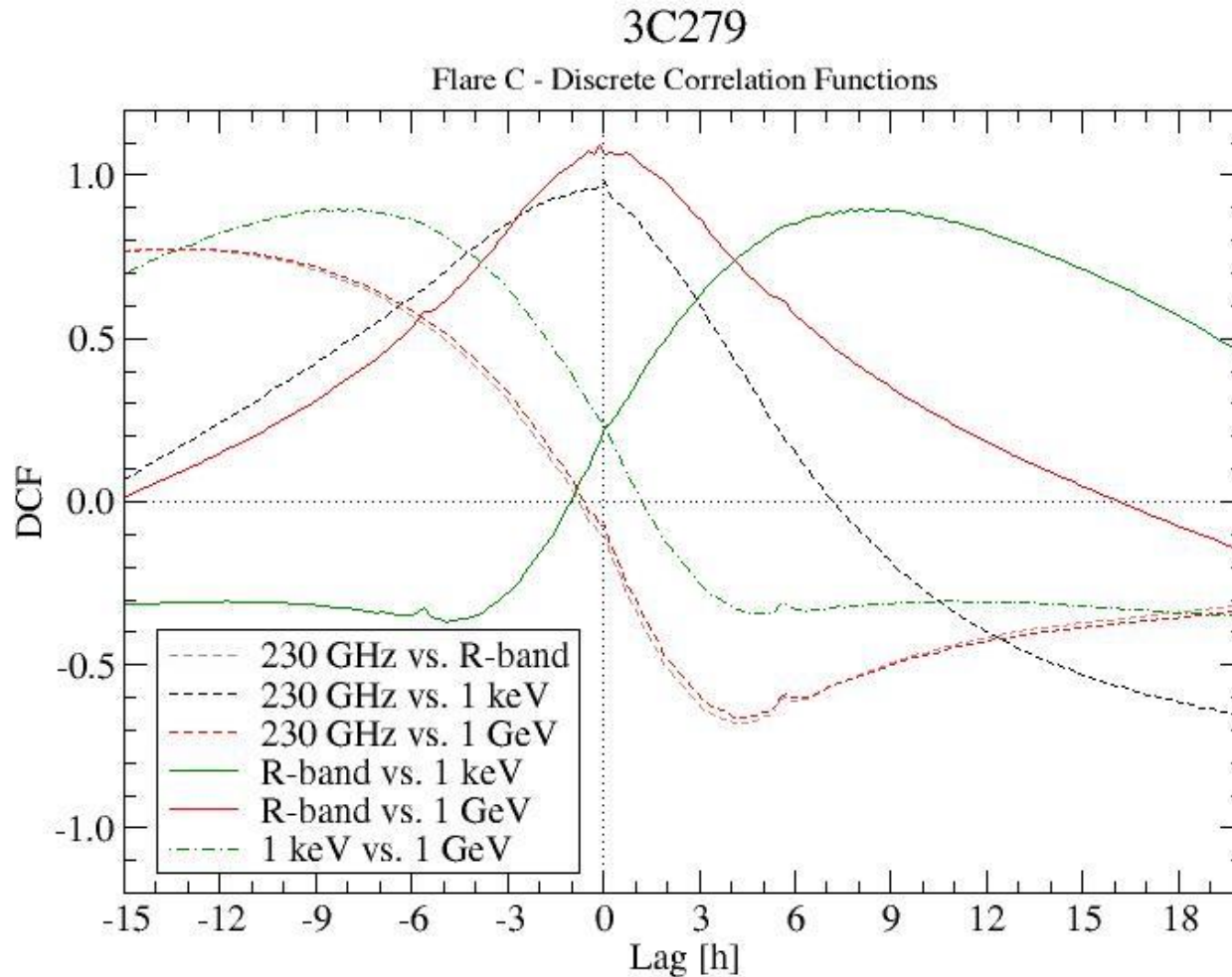
# 3C279 – Flare C

## Hardness-Intensity Diagrams



# 3C279 – Flare C

## Discrete Correlation Functions



- Optical and  $\gamma$ -rays well correlated (0 lag)
- X-rays and radio well correlated (0 lag)
- X-rays and radio lag optical +  $\gamma$ -rays by  $\sim 7 - 9$  hr)